

---

# IMPROVEMENT OF THE VISCOELASTIC PROPERTIES OF AC-20 ASPHALT BY APPLYING LOCAL NANO CLAY IN HMA MIXES

---

Ignacio Bladimir Cerón-Guerra, Guillermo Loría-Salazar, María José Cerón, Mariela Macias, Raúl Rodríguez and Giovanni Sáenz-Arce

## SUMMARY

The objective of this work is to improve the viscoelastic properties of local AC-20 asphalt. Ecuador has a nano clay deposit arranged in 6 levels from A1-A6, in an area of 4000 km<sup>2</sup>. Those nano clays were treated with chemical and physical methods, using a) NaOH, b) NH<sub>3</sub>, H<sub>2</sub>O<sub>2</sub> (molar ratio 5), and c) calcination to obtain an effective additive to be mixed with the bitumen. 532 samples were prepared, and their viscoelastic properties were measured with the dynamic shear rheometer (DSR) in the first stage. In the second stage, the best hot mix asphalt (HMA) samples were selected, and the parameters of mixing time, mixing

speed, calcination temperature, and additive concentration were optimized. It was discovered that nano clay A1 calcined in the 270-275°C window activated its high level of adsorption, becoming the best additive (SI) for HMA hot asphalt mixtures. The use of 3% SI + AC-20 and mixing times (MT) of 30, 60, 90 and 120 minutes allowed the complex modulus ( $G^*$ ) to increase up to 305.5%, while the phase angle  $\delta$  decreased by -8.37% (MT= 90 min). The performance grade improved from PG= 64 (original) to 70, 76, and 82. These results agree with the significant adsorption capacity that this material presents.

---

## Introduction

The present research is based on modifying the asphalt binder with local nano clay to protect it against rutting and cracking at high and medium temperatures. Ecuador has the raw material for this research, that is, it has nano clays that were used as a modifying additive from the Santo Tadeo geological formation in the central area of the province of Santo Domingo de Colorados de Sachilas in Ecuador (Kaufhold *et al.*, 2009), and the local AC-20

asphalt of the Esmeraldas State Refinery. The research focused on two points: a) process, synthesize and determine the best local nano clay additive for HMA, among all samples taken in the field, b) optimize the best integration conditions of this selected additive to the asphalt, in order to obtain fundamental improvements of the viscoelastic properties of hot mix asphalt, HMA. For this purpose, they were chemically or physically treated, dehydrated, organic material removed, ground, and integrated into the asphalt,

during the preparation of multiple HMA samples and evaluated with the DSR. In this next section, a transfer of the best additive that generated rheologically superior samples was carried out; In addition, the study of the improvement of the PG was undertaken by varying the preparation parameters of the mixtures, with respect to: a) mixing time (MT); b) calcination time of the nano clay additive (CT); c) stirring speed, RPM and d) percentage of the additive, %S by weight, with respect to the mass of bitumen.

As a result of this analysis, a type of nano clay A1 was detected and by preparing the respective additive and integrating it into the asphalt, a modified mixture with a high degree of performance (PG) was achieved. Knowing that asphalt pavement failures occur in the three components of its conventional system: oxidation and environmental effects, quality of the mixture and subgrade structure; these modified asphalts studied here could be a solution for roads in medium and high temperature climates.

---

## KEYWORDS / Additive SI/ Asphalt / Dynamic Shear / Nano Clay / PG /

Received: 02/14/2024. Modified: 03/30/2024. Accepted: 04/15/2024.

**Ignacio Bladimir Cerón-Guerra** (Corresponding author). Master in Petroleum Exploration and Exploitation, IFP Energies nouvelles (IFPEN), France. Doctorate in Natural Sciences for Development (DOCINADE), Instituto Tecnológico de Costa Rica, Universidad Nacional de Costa Rica and Universidad Estatal a Distancia, Costa Rica. Consultant and Researcher, Senescyt, Quito. Dirección: e-mail: ivcgoill@gmail.com. ORCID: <https://orcid.org/0000-0002-6373-9772>.

**Luis Guillermo Loría Salazar**. Doctor in Civil Engineering,

University of Nevada, Reno, United States. Vice Chancellor of UIN Research, Universidad Isaac Newton, San José, Costa Rica. President of the International Society of Asphalt Pavements (ISAP). e-mail: lloria@uin.cr. ORCID: <https://orcid.org/0000-0002-2336-9703>

**María José Cerón Sarmiento**. Petroleum Engineer, Escuela Politécnica Nacional, Quito, Ecuador. Senior Reservoir Development Engineer, Latin America Latam, Schlumberger International, Quito, Ecuador. e-mail: maria.ceron1998@gmail.

com. ORCID: <https://orcid.org/0000-0002-5665-8755>.

**Mariela Macias Parraga**. MSc in Soil Mechanics and Geotechnical Engineering, Universidad Politécnica de Madrid, Spain. Road Consultant and Researcher, Ministry of Transportation and Public Works, Ecuador. e-mail: mjmp77@gmail.com. ORCID: <https://orcid.org/0000-0002-2454-4139>.

**Carlos Raúl Rodríguez**. PhD in Project Management, Construction Engineering and Sustainable Construction, University of Florida, United States. FICT

Principal Professor-Co-Director, Escuela Superior Politécnica del Litoral, ESPOL, Guayaquil, Ecuador. e-mail: crodrigu@espol.edu.ec. ORCID: <https://orcid.org/0000-0001-8915-0539>.

**Giovanni Sáenz-Arce**. PhD in Nanoscience and Nanotechnology, Universidad de Alicante, Alicante, Spain. Director and Researcher, Universidad Nacional de Costa Rica and Universidad de Murcia, Spain. e-mail: giovanni.saenz.arce@una.ac.cr. ORCID: <https://orcid.org/0000-0003-1848-7980>.

## MEJORA DE LAS PROPIEDADES VISCOELÁSTICAS DEL ASFALTO AC-20 MEDIANTE LA APLICACIÓN DE UNA NANOARCILLA LOCAL EN MEZCLAS DE HMA

Ignacio Bladimir Cerón-Guerra, Guillermo Loría-Salazar, María José Cerón, Mariela Macias, Raúl Rodríguez y Giovanni Sáenz-Arce

### RESUMEN

El objetivo de este trabajo es mejorar las propiedades viscoelásticas del asfalto local AC-20. Ecuador cuenta con un depósito de nanoarcilla dispuesto en 6 niveles de A1-A6, en un área de 4000km<sup>2</sup>. Estas nanoarcillas fueron tratadas con métodos químicos y físicos, utilizando a) NaOH, b) NH<sub>3</sub>, H<sub>2</sub>O<sub>2</sub> (relación molar 5), y c) calcinación para obtener un aditivo eficaz para mezclar con el bitumen. Se prepararon 532 muestras, cuyas propiedades viscoelásticas se midieron con el reómetro de corte dinámico (DSR por sus siglas en inglés) en la primera etapa. En la segunda etapa, se seleccionaron las mejores muestras de mezcla asfáltica en caliente (HMA por sus siglas en inglés) y se optimizaron los parámetros de tiempo

de mezcla, velocidad de mezcla, temperatura de calcinación y concentración de aditivo. Se descubrió que la nanoarcilla A1 calcinada en un rango de temperatura de 270-275°C, activaba su alto nivel de adsorción, convirtiéndose en el mejor aditivo (SI) para las mezclas asfálticas en caliente HMA. El uso de un 3% de SI + AC-20 y tiempos de mezcla (MT) de 30, 60, 90 y 120 minutos; permitió aumentar el módulo complejo (G\*) hasta un 305,5%, mientras que el ángulo de fase  $\delta$  disminuyó un -8,37% (MT= 90 min). El grado de rendimiento mejoró de PG= 64 (original) a 70, 76 y 82. Estos resultados concuerdan con la importante capacidad de adsorción que presenta este material.

## MELHORIA DAS PROPRIEDADES VISCOELÁSTICAS DO ASFALTO AC-20 COM A APLICAÇÃO DE NANOARGILA LOCAL EM MISTURAS DE HMA

Ignacio Bladimir Cerón-Guerra, Guillermo Loría-Salazar, María José Cerón, Mariela Macias, Raúl Rodríguez e Giovanni Sáenz-Arce

### RESUMO

O objetivo é melhorar as propriedades viscoelásticas do asfalto AC-20 local. O Equador tem um depósito de nanoargila disposto em seis níveis, de A1 a A6, em uma área de 4.000km<sup>2</sup>. Essas nanoargilas foram tratadas com métodos químicos e físicos, usando a) NaOH, b) NH<sub>3</sub>, H<sub>2</sub>O<sub>2</sub> (razão molar 5) e c) calcinação. Para obter um aditivo eficaz para ser misturado ao betume. Foram preparadas 532 amostras, e suas propriedades viscoelásticas foram medidas com o reômetro de cisalhamento dinâmico (DSR) no primeiro estágio. Na segunda etapa, as melhores amostras de asfalto misturado a quente (HMA) foram selecionadas, e os parâmetros de tempo de mistura, velocidade de

mistura, temperatura de calcinação e concentração de aditivo foram otimizados. Descobriu-se que a nanoargila A1 calcinada na janela de 270 a 275°C ativou seu alto nível de adsorção, tornando-se o melhor aditivo (SI) para misturas de asfalto quente HMA. O uso de 3% de SI + AC-20 e tempos de mistura (MT) de 30, 60, 90 e 120 minutos permitiu que o módulo complexo (G\*) aumentasse em até 305,5%, enquanto o ângulo de fase  $\delta$  diminuiu em -8,37% (MT= 90 min). O grau de desempenho melhorou de PG= 64 (original) para 70, 76 e 82. Esses resultados estão de acordo com a capacidade de adsorção significativa que esse material apresenta.

There are some successful studies in the world, with the modification of bitumen with nano clay additives. These problems were addressed in earlier times, so in the 1950s, asphalt cement was initially used in the United States by heating bitumen and mixing it with aggregate to form Hot Mix Asphalt, or HMA (Roberts *et al.*, 1991a). In 1987, the Strategic Highway Research Program (SHRP) was launched to develop tests for asphalt binders and HMA mixtures. In 2003, the Federal Highway Administration (FHWA) defined functional and structural failures of

pavement. These three faults produce functional and structural problems on the highways (Miller *et al.*, 2003). In 2004, with the DSR, the resistance to rutting at high temperatures was determined in samples of different asphalt binders until finding those with high performance based on previously prepared nano clay (Airey *et al.*, 2004). In 2012, tests were carried out on asphalt mixtures with montmorillonite nano clays as a mineral additive to improve resistance to rutting and fatigue cracking using unmodified nano clays (NMN). At the same time, samples modified with polymers (PMN)

were prepared and added in concentrations of 2% and 4% by weight to the asphalt binder (Yao *et al.*, 2012). Another study in 2013 found that binder modification with nano clays led to increased viscosity and performance at high temperatures due to the high rigidity of the asphalt binder (Onochie, Yang, and Mills-Beale, n.d.). In 2018, previous research focused on improving the asphalt binder with styrene butadiene styrene (SBS), elvaloy, ethyl vinyl acetate (EVA), and ethylene styrene interpolymer (ESI), but Cloisite 20 nano clay was also used to improve the rheological properties of the asphalt binder

(Hu *et al.*, 2019). In 2022, the nano clay-Al<sub>2</sub>O<sub>3</sub> compound was studied for the intermediate and high-temperature properties of pure and modified asphalt binders and their effect on hot asphalt mixes (Mamuye *et al.*, 2022).

### Materials and Methods

#### Characterization materials

The materials are a) AC-20 asphalt from the Esmeraldas State Refinery, and its characterization was carried out in the refining laboratory of the State Refinery (Laboratorio de Control de Calidad de La

Refinería Esmeraldas: Calidad en sus Productos – EP Petroecuador, whose results are shown in Table I. b) The nano-clay was obtained directly from the clay deposits of the geological horizons A1, A2, A3, A4, A5 and A6, of the San Tadeo formation in the province of Colorados de Tsáchilas in Ecuador (0°14'14.13' 'S; 79° 14'27.05''E) (Figure 1). The microscopic and nanometric characterization of the nano clays were carried out in the Extractive Mineralogy Laboratory and Faculty of Chemistry, National Polytechnic School (Escuela Politécnica Nacional | Departamento de Metalurgia Extractiva (DEMEX)) the results of which are shown in Table I. The data obtained show the characteristics of nanometric material: a) nanometric particles, matter with a size between 50 and 250 nanometers; b) a specific surface area of 280m<sup>2</sup>/gr; and c) a high adsorption property. The chemical composition corresponds to aluminum and silicon oxides structured in tetrahedrons and octahedrons, generating laminar structures of the material (Kaufhold *et al.*, 2009). Each nano clay was name with A, and its respective additive (S) product name with S, therefore: A1 (S1), A2 (S2), A3 (S3), A4 (S4), A5 (S5), and A6 (S6).

#### Preparation of different additives

In this first stage, three methods were developed to obtain nano clay additives to enter the asphalt mix, as follows:

Method 1: Compound additive, 75 molar (75M) solutions were prepared with diesel 2 + nano clay (previously treated with H<sub>2</sub>O<sub>2</sub> and dehydrated at 105°C). It was homogenized for 30 minutes, and 30 minutes later it was subjected to sonication at 40,000Hz (waterproof kit, SkyMen JP-020S Cleaning). The syrups were added to the HMA in mixture 1.

Method 2: Additive prepared based on nano clay that is treated with NaOH or NH<sub>3</sub> (5M), with the purpose of

AC-20 Asphalt			Nano Clay	
Vitreous temperature (°C)	70		Calcination temperature (°C)	20 – 1000
Liquid phase temperature (°C)	160		Baking temperature Gradient (°C/min)	0.095
Volume (cm <sup>3</sup> )	350.7		Chemical concentration (M)	0/5
Type PG	64-22		Chemical type	NaOH, NH <sub>3</sub> , H <sub>2</sub> O <sub>2</sub> , HCl
Characteristics (accredited laboratory No. OAE LE-C13 002)			Crushing type	Mortar/EQ AC-CZ-4500rpm
Absolute viscosity (60°C) Pa·s	ASTM D2171-NTE	200	Calcination mass (g)	40
Kinematic viscosity (135°C) (mm/s)	ASTM D2170-NTE	369	Chemical composition	SiO <sub>2</sub> -Al <sub>2</sub> O <sub>3</sub> (Si, Al, Fe, Mg)
Penetration (25°C 100G 5s) (dmm)	ASTM D5-NTE	75	Density (gr/cm <sup>3</sup> )	2.65
Flashpoint (°C)	ASTM D92-NTE	288	DRX	Quartz, montmorillonite and actinolite
Solubility in trichlorethylene (%)	ASTM D2042-NTE	99.9	IFTR	group: OH, O-Si-O, O-Al-O, MO
Viscosity (60°C) (Pa·s)	ASTM D2171-NTE	672	Laser granulometry (nm)	50-250
Ductivity (25°C) 5cm/min	ASTM D113-NTE	67	SEM	globular, concentrations px
API gravity (15.6°C)	ASTM D1298-NTE	7.8	TGA (%)	loss of mass, 20-40
Relative density (15.6/15.6°C)	ASTM D1298-NTE	1.0202	DT	Endothermic and exo-thermic
Specific gravity (25/25°C)	ASTM D70	1.0113	DTA	elimination of organic matter / OH
Softening point (°C)	ASTM D36	49	Chemical analysis	Si, Al, Fe
Mass change (%)	ASTM D2872	-0.26	BET, samples (m <sup>2</sup> /gr)	207.83/280.38 and 223.62/221.85
Penetration index	ASTM D5	-0.5	SPECMIN/TSG	allophane, vermiculite, bentonite

PG: Performance Grade.

activating this material. The process carried out in solgel solutions and rinsing, which generated significant volumes

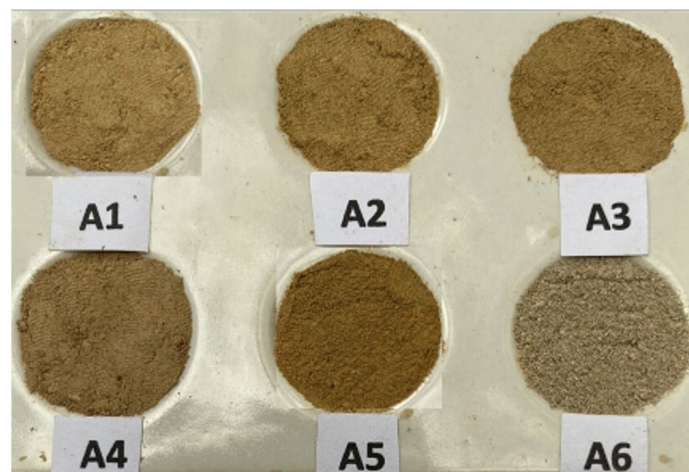


Figure 1. Palette of samples of the nano clay formations (A1-A6).

of wastewater, maintained a maximum pH of 6 to 9 (evaluated with ATC Ec/pH equipment). The dehydration process times at 105°C reached 80 hours, which makes the method more expensive for industrialization projects (Alshameri *et al.*, 2018) (Hakamy *et al.*, 2015).

Method 3: Additive obtained from the physical process of controlled calcination; a prior dehydration process was applied to the nano clay at 105°C, and then it was entered into the muffle to be calcined at an average temperature of 275°C. The nano clay at this temperature was able to eliminate organic matter and maintain its tetrahedral and octahedral structures, as well as its

specific surface area and important level of adsorption (Hakamy *et al.*, 2015), (Alujas *et al.*, 2015).

#### Muffle furnace

The SAFATHERM STM8-12 muffle is the equipment used to calcinate the nano clays and has the following characteristics: the maximum temperature reaches 1650°C, with Molybdenum disilicon resistors (MoSi<sub>2</sub>-SuperKanthal) and an A-304 stainless steel furnace casing; the temperature sensors are type S and B thermocouples with cooling in the electrical part by fan. The equipment is assisted with automated control with P0415 digital control and temperature ramp programmer with processor with solid data memory. The electrical supply is 220V and has a capacity of 1l. The samples to be calcined (20°C–350°C–1000°C) must be previously dehydrated, characterized, weighed, and placed in a sample holder according to the sample entry protocol and the temperature ramp plan to be submitted (“Muffle Furnace, Laboratory Muffle Furnace - Henan Sante Furnace Technical Co, Ltd.”).

#### Mixer homogenizing equipment

The integration of the nano clay S with the AC-20 binder was carried out using the AES500SH homogenizer equipment (high speed up to 14000RPM), assisted by a control panel, a stainless-steel mixing head, high cutting, and shearing. The temperature of the mixing container was kept constant at 160°C (to avoid thermal degradation of the AC-20), whose temperature was monitored by B thermocouples of the Osaka QB-32 processor + 220 V thermal sleeve. According to a protocol, the asphalt must be previously heated to 60°C. The temperature at which the asphalt flows and 400g of betumen were measured on a BOECO-Germany-Instruments high precision balance system (0.001g sensitivity), and the additive

was also weighed in percentage by weight, according to the test plan. The binder is carried at a speed of 4500RPM with the mixing temperature, and the respective additive is entered in a constant manner together with the vortex formed in the container. Then continue with the homogenization for the corresponding time, where at least 2 hours will be taken. Samples were taken to the asphalt rheology laboratory in preserved form (“AE500S-H Homogenizer High Shear Mixer Emulsifying Machine Digital Display (90G/60L): Amazon.Com: Tools & Home Improvement).

#### Dynamic shear rheometers (DSR)

Perform the critical rheological characterization analysis required for the Super Pave PG (performance grade), classification of asphalt binders. The DSR test uses a thin asphalt binder sample sandwiched between two circular plates. The lower plate is fixed while the upper plate oscillates back and forth across the sample to create a shearing action.

The 81-PV6202 DSR model performs Super Pave Performance Grading according to AASHTO T315 and ASTM D7175, Viscosity Determination of Asphalt Binder according to AASHTO

T316 and ASTM D4402, and Multi-Stress Creep Recovery (MSCR) according to AASHTO T350 and ASTM D7405.

The fundamental services are:

- PG determination test
- Determination of deformation properties of bitumen with the Multiple Stress Creep Recovery Test (MSCR).
- Determination of the complex shear modulus  $G^*$  and phase angle  $\delta$  of road bitumen at different temperatures.
- DSR tests are conducted on unaged, RTFO-aged, and PAV-aged asphalt binder samples. The binder behavior under various temperature and loading conditions is analyzed to predict its performance under anticipated climatic - With automatic gap setting. 110-220V, 50-60Hz, 1pH.

The tests were carried out with HMA mixtures whose shear dynamic modulus is between 100Pa and 10MPa at a temperature of 70°C and an angular frequency of 10rad/second, using a sinusoidal waveform. The test specimens were 1mm thick by 25mm in diameter and were tested between parallel metal plates. During the test, one of the parallel plates oscillates with respect to the other at a preselected frequency and rotational strain amplitudes (strain-controlled) or shear amplitudes (stress-controlled). The

required amplitude depends on the value of the complex shear modulus of the tested asphalt. The required amplitudes have been selected to ensure that the measurements are within the region of linear behavior. The asphalt specimen is maintained at the test temperature within  $\pm 0.1^\circ\text{C}$  by heating and cooling the upper and lower plates. The test specification is for a test frequency of 10rad/second. The  $G^*$  and the  $\delta$  are automatically calculated as part of the rheometer operation using computer software supplied by the equipment manufacturer (Bohlin). The complex shear modulus is an indicator of the stiffness or resistance of the asphalt binder to deformation under load. (Table II).

The data obtained were  $G^*$  and  $\delta$ , provided by the rheometer. These parameters allow us to estimate the rutting factor,  $\text{RF} = G^* \sin \delta$ , and the PG, showing the viscoelastic properties of the modified asphalt binder, HMA.

#### Definition of the reference level of PG measurement

The assumed methodology was the measurement of the PG of all the HMA samples, obtained with the 3 types of additives previously prepared, and a trend of positive results was outlined. A reference level was established for the measurement

TABLE II  
DSR, TECHNICAL SPECS

Rheometer 81-PV6202			
Torque Range (mNm)	0.1 to 150	Normal force range (N)	-30 to 30
Torque resolution (mNm)	0.001	Normal force resolution(N)	0.01
Speed Range rpm	0 to 2000	Automatic gap setting	Yes
Speed Resolution rpm	0.015	Gap resolution ( $\mu\text{m}$ )	1
Viscosity Range, RN general (mPa·s)	1 to $1 \times 10^{10}$	Temperature control unit	
Viscosity Range, plate P3 (mPa·s)	$1 \times 10^2$ to $1 \times 10^8$	Maximum temperature ( $^\circ\text{C}$ )	180
Viscosity Range, plate P4 (mPa·s)	$5 \times 10^3$ to $1 \times 10^{10}$	Minimum temperature ( $^\circ\text{C}$ )	-15
Complex Shear Modulus, plate P3 (kPa)	$0.1$ to $2 \times 10^4$	Temperature accuracy (K)	$\leq 0.1$
Complex Shear Modulus, plate P4 (kPa)	$20$ to $4 \times 10^6$	Range $5^\circ\text{C}$ to $90^\circ\text{C}$	
Phase Angle Range	$0$ to $90^\circ$	Interface	USB 2.0
Frequency (Hz) 0,001 to 100		Plats (mm)	25

of viscoelastic properties with the DSR in order to select the additive with the greatest impact on the HMA, with the highest performance. It was defined that the fixed reference level of the RF value was designated as the Performance Reference Level (PRL), which is equal to or greater than 1.0Kpa, maintaining the test temperature in the DSR at 70°C. (PG= 70); Therefore, all HMAs will be compared with this reference and may achieve lower or higher PG (the values are of our interest).

### Nomenclature of the HMA

To organize the results of the HMA with the 3 different additives previously pre-primed with the homogenizer and evaluate their new rheological properties, a nomenclature was adopted that carries sufficient information on the conditions of mixing time, sonication, calcination, percentage of additive, type of additive, and number of repetitions of the experiment under similar conditions. Next, we expose it to:

*B3S6-90 30 N1 R1*  
(Example of the name of one HMA mixture)

Where the formulation means:

1: (B) Indicates the type of additive treatment that was used in the mixture:

- A: natural nanoclay with H<sub>2</sub>O<sub>2</sub> and dehydrated
- B: nanoclay synthesized with NaOH.
- C: nanoacly synthesized with NH<sub>3</sub>.

2: (3) Indicates the percentage by weight of S in the mixture.

The mass ratios of S (weight percentage with respect to asphalt) were measured with the BOECO Germany brand BPS 40+.

3: (S6) Indicates the type of additive (S6 in this case) and physical state of the solute used:

- S: additive in solid.
- J: additive in syrup.

4: (90) Indicates mix time with the homogenizer (HMA), which has each sample, MT.

5: (30) Indicates the ultrasound time imposed on the HMA, ST.

6: (N1) Indicates the dehydration / calcination temperature of additive:

- N1: S calcinate between 20 and 365°C, CT.

- N2: S calcinate between 365 and 1000°C, CT.

- N3: S at 10 Molar Chemical Concentration.

7: (R1) Indicates the replica number (repetition) of the sample HMA; the first sample will not appear; it will only be used from the first replica: R1, R2, successively.

### Selection of the additive by HMA performance results

The name of each HMA sample was established under the nomenclature indicated above, in which the parameters of mixing speed (4500RPM) and temperature (160°C) were kept constant. The prepared mixtures are divided into 3 groups: a) Mix 1, additive (J, S1,2,3..6)+ AC-20 and sonicated for 30min; b) Mix 2, additive (S+ chemicals; S1,2,3..6) + AC-20; and c) Mix 3, additive (S calcination, S1,2,3..6) + AC-20 asphalt. The universe of samples evaluated totaled 532 (Figure 2). The RF value of each sample was compared with the PRL reference value established as the reference level of PG 70, and those with a higher value were counted as positive. Finally, in this phase, the best additive Si (one or more additives) could be determined, which generated more samples with high RF and PG. (Iskender, 2016).

### HMA optimization with additive of choice S

With the selected additive Si (i=1,2,3..6) the optimization of the HMA mixtures was carried out, for which control of RF results was carried out, of multiple samples, each time varying the following variables in an orderly manner: a) %S; b) CT; c) RPM; and d) MT; This process was structured in the process flowchart, explained in Figure 3. 162 new HMAs were obtained, which were repeated and evaluated considering the various mixing configurations. Groups I, II, III and IV were organized and labeled, which contain classes of modified asphalt mixtures from A to N. The final objective was to determine the HMA samples with high RF value, and determine the operating conditions and parameters followed by mixing. The complex modulus G\* and the phase angle were evaluated with the DSR, in an iterative manner of repeated mixtures, until the best values of the rheological variables were achieved, with high PG (Firouzinia and Shafabakhsh, 2018; Jahromi, 2009).

## Results

### Evaluation of G\* and δ

The 6 nano clays were processed by chemical and thermal methods (treated with

NH<sub>3</sub>, NaOH, H<sub>2</sub>O<sub>2</sub> and calcination), then 3 groups of additives were prepared: a) J (chemically treated nano clay + diesel), b) S (chemically treated nano clay) and c) S<sub>c</sub> (calcined nano clay). These additives were homogenized with AC-20 asphalt in HMA, according to the methodology explained above, then their new viscoelastic properties were measured with the DSR at 10Hz and 70°C (reference PRL= RF= 1Kpa, PG= 70). The following results were obtained: a) Mix 1. 100% of the HMA mixtures that contained additive J did not exceed the PRL; b) Mix 2. 24.6% of the HMA mixtures with the additive S + chemicals if they exceeded the PRL; c) Mix 3. 84.8% of HMA mixtures prepared with calcined S additive exceeded the PRL reference level, in addition 3.2% of these mixtures reached new values at PG 76 and 82 (Figure 4 and Table III).

### Selection of additives and final mixtures HMA

In the previous section, it was possible to segment the best HMA mixtures, which included additives from type A1 and A2 nano clays, such as controlled calcination and more favorable preparation and mixing methods; However, the additive from the A1 nano clay improved the rheological properties in more than 90% of

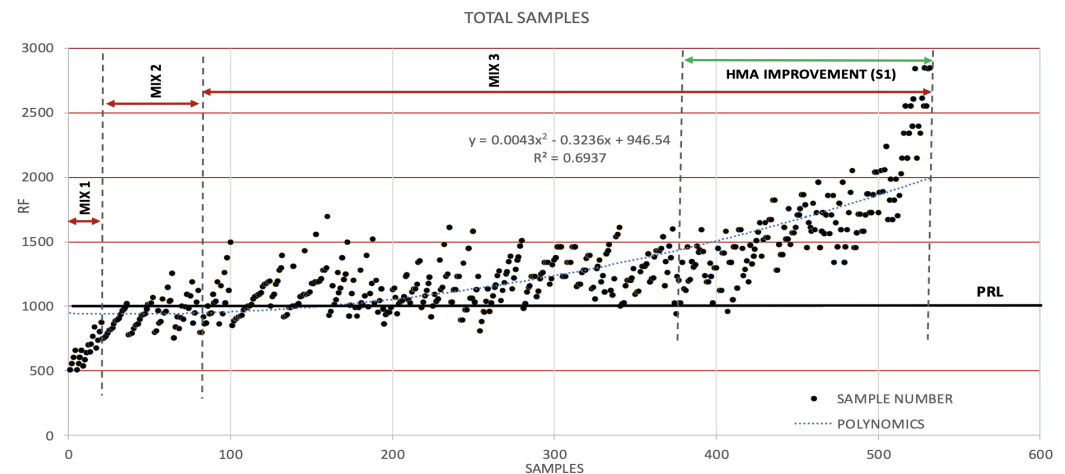


Figure 2. Universe of the evolution of HMA improvement, RF(Pa).

**Additive (S) selection method and final mixes PG**

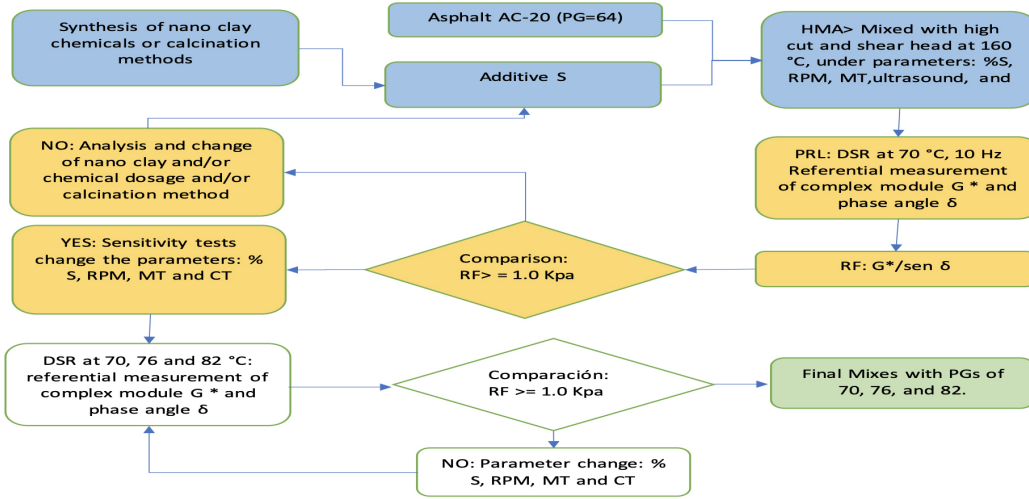


Figure 3. Scheme to optimize mixtures of additive and binder.

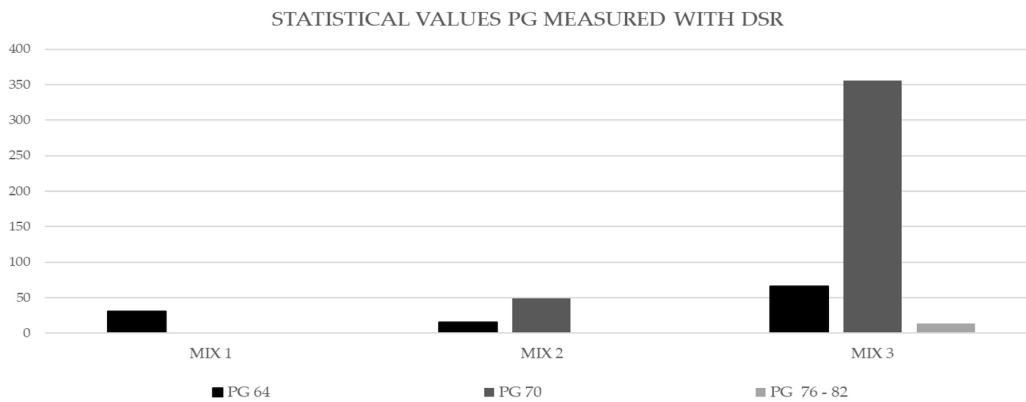


Figure 4. Mixture success percentages (HMA) and PG were evaluated with DSR.

**TABLE III**  
**PG EVALUATION OF HMA SAMPLES**

PG	Mix 1	Mix 2	Mix 3	Total
64	177	153	23	
70		50	124	
76-82			5	
	177	203	152	532

PG: Performance Grade.

cases. Another element that was detected was the sensitivity process of rheological results depending on the variation of mixing parameters, such as time, speed, percentage of additive and its preparation. Thus, in this work we also worked to form a map of results by varying these faces

in order to achieve modified asphalts with the highest possible PG Next, Table IV and Figure 5.

*RF and PG improvement by optimizing mixing parameters*

It was proposed to optimize the HMA mixtures and obtain

the best PG, for which the additive S1 (nano clay A1 calcined at 275°C) was selected with which sets of samples labeled from A to N and grouped in 4 groups I, II, III and IV according to the mixing surfaces, which varied in the experimentation Table V. The obtains results below:

**Group I**

In the evaluation of the samples of classes A, B, and C of HMA, the variation of the parameters  $G^*$  and  $\delta$  was observed when progressively entering the additive S1 in the percentages 2%, 3%, 5%, 8%, 10%, and 11% (Figure 6). The parameters RPM= 4500, CT= 275°C, and M= 160°C were kept constant. 3 mixtures with S1 of 3%, 8%, and 11% were the most representative, with the following results:

1) Class A (MT= 30 min), the HMA samples with 3%, 8%, and 11% S1 presented a substantial increase in  $G^*$  and decreases in  $\delta$ , highlighting the mixture with 11%,  $G^*= 1459.9$  Pa, and  $\delta= 81.2^\circ$ ; however, with a smaller amount of additive S1= 3%,  $G^*= 1135.5$  Pa and  $\delta= 81.2^\circ$  were obtained, and a more elastic asphalt binder was obtained than the original AC-20,  $G^*= 605.5$  Pa and  $\delta= 84.8^\circ$ , and with an improvement in the RF. The parameters of the aggregates S1= 3% and 11% were compared, with a percentage increase in  $G^*= 22.2\%$  the mixture with more additive S1.

2) Class B (MT= 60 min), the HMA samples with S1= 3%, 8%, and 11% maintained substantial increases in  $G^*$  and decreases in  $\delta$ , standing out the mixtures with 3% and 11%,  $G^*= 1570.7$  Pa and  $\delta = 79.3^\circ$  and  $G^*= 1863.6$  Pa and  $\delta= 79.4^\circ$ , respectively. However, the samples obtained with an additive less than S1= 3% have a binder as rigid and more elastic as that of S1= 11%, but with a  $G^*$  percentage greater than 15.72% and  $\delta= 0.126\%$ .

3) Class C (MT= 90 min), the HMA samples with S1= 3% and 11% further increased the values of  $G^*$  and decreased  $\delta$ , in  $G^*= 1849.0$  Pa and  $\delta= 77.7^\circ$  and  $G^*= 2240.5$  Pa and  $\delta= 77.9^\circ$ , respectively; the sample S1= 11% exceeded the parameter  $G^*$  by 17.46% compared to that of S1= 3%, at  $\delta= 0.256\%$ .

In general, it is established that the HMA sample of S1=

TABLE IV  
CONTINUOUS IMPROVEMENT OF HMA  
HMA OPTIMIZED PG WITH S1 ADDITIVE

#Muestra	Code	G*(Pa)	$\Delta(^{\circ})$	RF (Pa)	TC( $^{\circ}$ C)
1	A3S130N1R20	473	80	480	275
2	A3S130N1R18	523	81	530	282
3	A2S130N1R17	531	82	536	282
4	ORIGINAL 1	605	85	607	
5	ORIGINAL 1	642	85	645	
6	ORIGINAL 3	605	85	608	
7	A2S160N1R17	667	82	673	282
8	A3S160N1R18	676	81	684	282
9	A1S10N1R21	737	81	747	320
10	A1S10N1R21*	737	80	747	300
11	A3S190N1R18	769	84	773	282
12	A2S190N1R17	776	79	790	282
13	A5S190N1R8	802	84	806	200
14	A2S130N1R28	889	84	894	300
15	A2S130N1R31	896	84	902	375
16	A2S160N1R30	901	83	907	350
17	A2S130N1R39	909	84	914	235
18	A2S160N1R28	929	84	935	300
19	A3S130N1R22	933	84	940	275
20	A2S130N1R29	938	84	944	325
21	A2S160N1R31	944	84	950	375
22	A2S160N1R39	944	83	951	235
23	A2S160N1R33	950	83	957	375
24	A2S130N1R40	951	83	958	220
25	A2S160N1R29	960	83	967	325
26	A5S190N1R49	963	82	974	275
27	A3S130N1R33	981	84	987	275
28	A5S130N1R10	994	83	1001	300
29	A2S130N1R42	1012	83	1020	250
30	A2S130N1R26	1028	82	1038	250
31	A5S130N1R3	1028	83	1037	136
32	A2S130N1R27	1033	83	1040	275
33	A3S130N1R34	1057	83	1066	325
34	A8S190N1R52	1062	82	1073	275
35	A8S190N1R52	1062	82	1073	275
36	A3S160N1R34	1077	83	1086	325
37	A3S130N1R21	1080	83	1089	275
38	A3S130N1R25	1090	82	1101	320
39	A5S190N1R3	1090	83	1098	136
40	A5S130N1R11	1091	83	1100	325
41	A2S160N1R27	1092	82	1102	275
42	A5S130N1R9	1092	83	1101	250
43	A5S130N1R12	1095	83	1104	300
44	A2S160N1R40	1097	82	1107	220
45	A2S130N1R63	1100	82	1110	275
46	A2S130N1R63	1100	82	1110	275
47	A3S130N1R41	1105	82	1115	275
48	A3S130ZN1R0	1114	82	1125	270
49	A3S110ZN1R0	1114	82	1124	240
50	A11S1120N1R54	1121	81	1137	275
51	A11S1120N1R54	1122	80	1137	275
52	A3S130N1R58	1134	81	1147	275
53	A2S130N1R48	1135	82	1146	275

3% generates very favorable values of  $G^*$  and  $\delta$ , which implies that a weight of 27.27%, compared to 100% by weight of S= 11 % generated an improvement in the binder, making it more rigid and elastic.

The viscoelastic change efficiency, VCE, defines the positive percentage of the increase in the magnitude of  $G^*$  and decrease in  $\delta$  when the variables are time MT and S%. In this study, the viscoelastic improvement of HMA is very promising with S1= 3%, and at a lower cost.

#### Group II

The evaluation of  $\delta$  and  $G^*$  of the samples of the classes D, E, and F is carried out with an increase in the calcination temperature of the nano clay, CT, at 200, 250, 275, 300, and 325 $^{\circ}$ C (5 different additives S1) and a MT of 30, 60, and 90min. The parameters of S1= 3%, RPM= 4500, and mixing temperature= 160 $^{\circ}$ C, were kept constant, with the following results:

1) In the samples of class D (MT= 30 min), corresponding to calcination temperatures of 200, 250, 275, 300, and 325 $^{\circ}$ C. The three most representative samples reached  $G^*$  values of 1192.9, 1174.3, and 1179.4 Pa, with an average decrease of  $\delta$  of 81 $^{\circ}$ . All the samples exceed PRL= 1Kpa, which represents PG 70 according to the scheme of Figure 7.

2) In the samples of class E (MT= 60 min). In particular, the sample prepared with the additive at the calcination temperature of 275 $^{\circ}$ C reached a  $G^*$  value of 1570.7Pa, and the  $\delta$  decreased on average to 79.3 $^{\circ}$ . All other samples are below these values in  $G^*$  and above the indicated  $\delta$ , as shown in Table V. The difference between these parameters and the sample from the same group is very noticeable.

3) In the samples of class F (MT= 90min), in the same way as the previous case, the most representative sample corresponds to the calcination temperature of 275 $^{\circ}$ C and

TABLE IV (Cont.)  
CONTINUOUS IMPROVEMENT OF HMA  
HMA OPTIMIZED PG WITH S1 ADDITIVE

#Muestra	Code	G*(Pa)	$\Delta(^{\circ})$	RF (Pa)	TC( $^{\circ}$ C)
54	A2S130N1R38	1136	82	1147	250
55	A2S130N1R38	1136	82	1147	240
56	A3S160N1R22	1138	81	1151	275
57	A3S130N1R15	1144	80	1160	225
58	A3S130N1R15	1144	82	1154	270
59	A3S130N1R24	1150	83	1158	300
60	A5S130N1R7	1169	81	1183	150
61	A3S130N1R50	1174	82	1185	250
62	A3S130N1R32	1174	82	1185	300
63	A3S130N1R14	1176	82	1188	200
64	A3S130N1R14	1176	82	1187	210
65	A3S130N1R51	1179	82	1190	325
66	A5S130N1R13	1189	82	1199	275
67	A3S130N1R23	1190	81	1206	280
68	A3S130N1R16	1193	83	1203	250
69	A3S130N1R57	1211	81	1226	275
70	A3S130N1R57	1212	81	1227	275
71	A3S630N1R100	1215	81	1230	270
72	A3S160N1R24	1220	81	1236	300
73	A3S630N1R103	1222	81	1236	180
74	A5S130N1R49	1227	82	1239	275
75	A10S130N1R53	1230	82	1243	275
76	A10S130N1R67	1230	82	1244	275
77	A10S130N1R53	1230	82	1243	275
78	A2S160N1R38	1233	82	1245	250
79	A3S130N1R13	1253	82	1265	275
80	A3S160N1R21	1280	83	1291	275
81	A3S160N1R32	1287	81	1302	300
82	A3S160N1R41	1323	81	1339	275
83	A3S160N1R23	1340	82	1353	280
84	A3S190N1R22	1354	82	1367	275
85	A3S160N1R14	1360	81	1376	200
86	A3S160N1R14	1360	81	1376	240
87	A2S160N1R42	1372	81	1389	250
88	A3S160N1R15	1375	82	1387	225
89	A3S160N1R15*	1375	81	1391	250
90	A5S190XN1R0	1375	83	1386	250
91	A5S190XN1R0	1375	81	1393	260
92	A3S160N1R25	1380	81	1398	320
93	A5S160N1R7	1384	81	1400	150
94	A3S160N1R50	1394	81	1411	250
95	A3S160N1R51	1395	81	1412	325
96	A2S160N1R63	1412	80	1432	275
97	A2S160N1R63	1412	80	1432	275
98	A2S160N1R26	1419	81	1439	250
99	A2S160N1R48	1430	81	1449	270
100	A2S160N1R48	1430	81	1449	275
101	A2S160N1R48	1430	81	1449	275
102	A5S160N1R11	1438	81	1458	325
103	A3S190N1R24	1450	81	1469	300
104	A11S130N1R54	1460	81	1477	275
105	A11S130N1R54	1460	81	1477	275
106	A11S130N1R54	1460	81	1477	275

reached the highest value of  $G^*$  of 1849 Pa, with an average decrease of  $\delta$  of  $77.7^{\circ}$ . All other samples are below these values in indicated  $G^*$  and above in  $\delta$ . It is concluded that the parameters  $CT=275^{\circ}C$  and  $S1=3\%$  generate a more optimized HMA with optimal viscoelastic properties.

### Group III

The parameters  $G^*$  and  $\delta$  are evaluated, which vary with the RPM advance up to 10,000 RPM and  $MT=30$  and  $60$  min for the G and H mixtures, respectively.  $S1=3\%$ ,  $CT=275^{\circ}C$ , and mixing temperature =  $160^{\circ}C$  were kept constant (Figure 8), with the following results:

1) In the samples of Class G ( $MT=30$  min), when increasing the speed in the head of the emulsifier with magnitudes between 2,800 and 10,000RPM, it was established that up to 4,500RPM (the mixing temperature of  $160^{\circ}C$  is maintained) there is laminar flow,  $G^*=1034.4$  Pa, and  $\delta=82.2^{\circ}$ . From 4500 to 6000RPM, an increase in the temperature of the mixture was found because of high speed, and it went from  $160^{\circ}C$  to  $178^{\circ}C$ . At 6000RPM, an exothermic process of the HMA mixture was generated, and the increase in molecular energy increased as well as the entry of air through the vortex produced in the binder with the corresponding oxidation. A high-temperature cracking aging of the mixture was determined when the temperature of the mixture reached  $227^{\circ}C$  at 10000RPM.

2) In the samples of Class H ( $MT=60$  min), when increasing the speed from 2800 to 10000RPM, as in the previous case, it was established that up to 4500RPM, the mixing temperature was maintained at a constant  $160^{\circ}C$ , verifying a laminar flow with values of  $G^*=1369.1$ Pa and  $\delta=80.4^{\circ}$ . From 4500RPM to 6000RPM, an increase in the temperature of the mixture was found due to the speed from  $160^{\circ}C$  to  $182^{\circ}C$ . At 6000RPM, an



TABLE IV (Cont.)  
CONTINUOUS IMPROVEMENT OF HMA  
HMA OPTIMIZED PG WITH S1 ADDITIVE

#Muestra	Code	G*(Pa)	$\Delta(\circ)$	RF (Pa)	TC( $\circ$ C)
107	A8S130N1R52	1463	81	1481	275
108	A8S130N1R52	1463	81	1481	275
109	A8S130N1R52	1463	81	1483	275
110	A8S130N1R52	1463	81	1481	275
111	A3S190N1R21	1467	81	1484	275
112	A3S160N1R12	1472	80	1494	300
113	A3S160N1R12	1510	79	1538	300
114	A3S160N1R12	1510	81	1527	300
115	A3S190N1R23	1520	82	1534	280
116	A11S1120N1R54	1524	80	1550	275
117	A11S1120N1R54	1524	80	1550	275
118	A3S160N1R16	1536	81	1555	250
119	A3S160N1R16	1536	81	1556	250
120	A3S160N1R11	1557	81	1576	275
121	A3S160N1R11	1557	82	1570	325
122	A3S190N1R51	1574	80	1599	325
123	A3S160N1R13	1582	80	1604	275
124	A3S160N1R13	1582	82	1599	275
125	A10S160N1R53	1591	80	1614	275
126	A10S160N1R53	1591	80	1614	275
127	A3S160N1R57	1592	79	1621	275
128	A3S160N1R57	1593	79	1622	275
129	A5S160N1R49	1596	81	1618	275
130	A5S1560N1R65	1598	81	1620	275
131	A3S160N1R13	1610	82	1626	275
132	A3S160N1R13	1610	81	1631	275
133	A3S190N1R50	1647	80	1672	250
134	A3S190N1R66	1648	80	1674	250
135	A2S190N1R63	1725	79	1755	275
136	A2S190N1R63	1725	79	1755	275
137	A3S160N1R58	1725	79	1760	275
138	A3S160N1R59	1725	79	1760	275
139	A2S190N1R48	1755	80	1785	275
140	A2S190N1R48	1755	79	1786	275
141	A8S160N1R52	1820	80	1849	275
142	A8S160N1R52	1820	80	1849	275
143	A5S190N1R49	1860	79	1893	275
144	A5S190N1R49	1860	79	1893	275
145	A3S160N1R101	1861	79	1899	255
146	A11S160N1R54	1864	79	1896	275
147	A11S160N1R68	1864	79	1896	275
148	A8S190N1R52	1960	79	1996	275
149	A8S190N1R59	1961	79	1995	275
150	A3S1590N1R57	1983	77	2032	275
151	A3S190N1R64	1983	77	2033	275
152	A8S190N1R58	2025	77	2076	275
153	A10S190N1R53	2039	79	2080	275
154	A10S190N1R58	2039	79	2080	275
155	A8S190N1R52	2049	79	2089	275
156	A8S190N1R62	2050	78	2093	275
157	A11S190N1R54	2241	78	2291	275
158	A10S1120N1R53	2552	77	2623	275
159	A10S1120N1R60	2554	77	2620	275

exothermic process of the HMA was generated due to the high speed. Premature aging due to high-temperature cracking of the mixture was observed, which reached 230°C at 10,000RPM. It was concluded that the ideal technical conditions for the speed of the mix, RPM, are 4500RPM, which ensures laminar flow and maintains the mix temperature at 160°C. If the percentage of the additive S1 is between the values of 3% and 5%, this condition can be altered upwards if the speed is maintained or lower.

#### Group IV

Classes I, J, K, L, M, and N are evaluated with parameters G\* and  $\delta$  with increasing MT of 30, 60, 90, and 120min for S1 of 2, 3, 5, 8, 10, and 11%. The values of CT= 275°C, 4500 RPM, and mixing temperature = 60°C were kept fixed. For all percentages of S1, G\* increases until reaching the maximum value of 2843.2Pa, and the phase angle  $\delta$  decreases to 76.9°, as a function of MT, at the maximum aggregate concentration of 11%. (Figures 9, 10).

#### Calculation of differentials of the parameters G\* and $\delta$

Table VII shows the calculated differentials of the variation of the parameters G\* and  $\delta$ , noted by  $\Delta G^*$  and  $\Delta \delta$ , which represent the excess values obtained by the improvement process AC-20 when incorporating the additive S1. Calculating RF, it was possible to know the PG with the following results:

- DSR at 70°C and RF  $\geq$  1Kpa, all groups passed (PG= 70).

- DSR at 76°C and RF  $\geq$  1Kpa passed groups L, M, and N (PG= 76).

- DSR at 82°C and RF  $\geq$  1Kpa approved only group N (PG= 82).

It is concluded that the MT mixing time is a variable that directly implies the increase of the parameters  $\Delta G^*$  and  $\Delta \delta$ .

TABLE IV (Cont.)  
CONTINUOUS IMPROVEMENT OF HMA  
HMA OPTIMIZED PG WITH S1 ADDITIVE

#Muestra	Code	G*(Pa)	Δ(°)	RF (Pa)	TC(°C)
160	A10S1120N1R53	2552	77	2620	275
161	A11S1120N1R54	2843	77	2922	275
162	A11S1120N1R55	2847	77	2927	275
Variance		179326	3	190700	
Standard Deviation		423	2	437	
Deviation Coefficient		0.31	0.02	0.32	

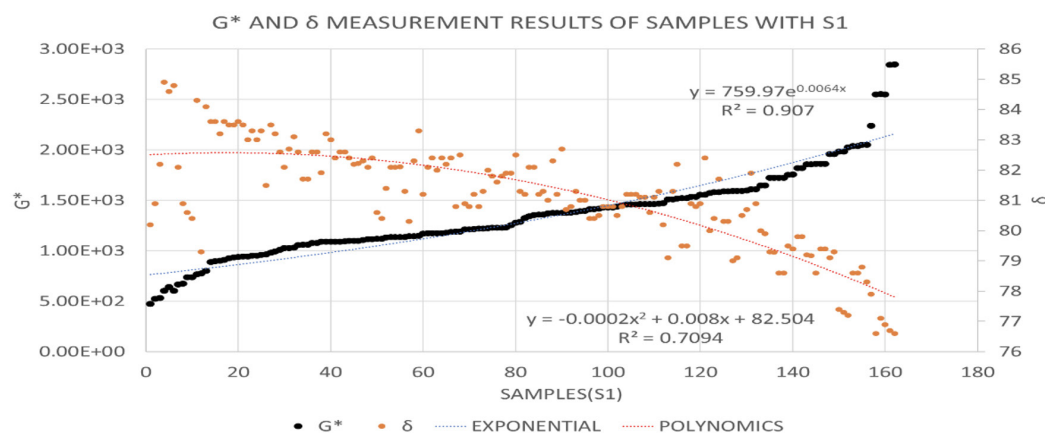


Figure 5. Evaluation of the results of viscoelastic parameters of improved HMA mixtures; G\*(Pa), δ (°).

For all cases, the parameters  $\Delta G^*$  and  $\Delta \delta$  also depend on the percentage of the additive (S1) that enters the HMA. If we seek to improve the binder to a PG= 70, it is recommended to use S1= 3% and MT= 60 min. due to the positive results of  $G^*= 1570.7$  Pa and  $\delta= 79.3$  ( $\Delta G^*= 67.28\%$  and  $\Delta \delta= 9.14\%$ ), which represent the first optimized values that appear in the mentioned table (Ezzat *et al.*, 2016).

## Discussion

The results obtained from successful HMA were based on the following elements: The purpose of the experimentation carried out was to take advantage of the nanometric properties of nano clay type A1, and work was done to activate its nanometric properties through the 3 methods of preparation of the additive, having categorical results with calcination under a window. The adsorption property of the nano clay was maximized and placed in contact with the hot AC-20 asphalt at 160°C, with very favorable results, in the improvement of its rheological

TABLE V  
EVALUATION OF HMA SAMPLES OF 14 CLASSES OF A-N; G\*(PA), Δ(°)

(%) S1	A		B		C		CT	D		E		F		
	δ	G *	δ	G *	δ	G *		δ	G *	δ	G *	δ	G *	
2	81.9	1054.8	80.1	1467.9	78.0	1830.6	200	82.0	1176.3	81.2	1360.1	79.9	1557.7	
3	81.2	1135.5	79.3	1870.7	77.7	1849.0	250	82.4	1192.9	80.8	1535.9	80.0	1646.6	
5	82.0	1226.7	80.5	1595.7	79.2	1859.6	275	81.2	1135.5	79.3	1570.7	77.7	1849.0	
8	81.1	1462.7	79.8	1820.1	79.1	1959.7	300	82.4	1174.3	81.3	1509.9	82.2	1520.0	
10	81.8	1230.2	80.3	1591.3	78.6	2038.6	320	81.9	1090.0	80.8	1380.0	80.8	1450.0	
11	81.2	1459.9	79.4	1863.6	77.9	2240.5	325	82.2	1179.4	81.0	1394.9	80.0	1574.3	
RPM	G		H				TM	I		J		J		
2800	83.3	778.66	82.7	872.57			0	84.8	605.05	84.8	605.05	84.8	605.05	
3500	82.1	1009.1	82.4	1092.1			30	81.9	1054.8	81.2	1135.5	82.0	1226.7	
4000	82.3	1032.6	81.1	1223.6			60	80.1	1467.9	79.3	1570.7	80.5	1595.7	
4500	82.2	1034.4	80.4	1369.1			90	78.0	1830.6	77.7	1849.0	79.2	1859.6	
5000	81.9	1054.8	80.2	1430.0										
5500	81.6	1085.0	80.2	1432.2										
6000	81.4	1134.9	80.1	1467.9										
8000	77.8	1658.4	77.3	2415.0										
10000	70.7	2375.9	72.5	3754.9										
								L		M		N		
								0	84.8	605.05	84.8	605.05	84.8	605.05
								30	81.1	1462.7	81.8	1230.2	81.2	1459.9
								60	79.8	1820.1	80.3	1591.3	79.4	1863.6
								90	79.1	1959.7	78.6	2038.6	77.9	2240.5
								120			76.9	2551.7	76.9	2843.2

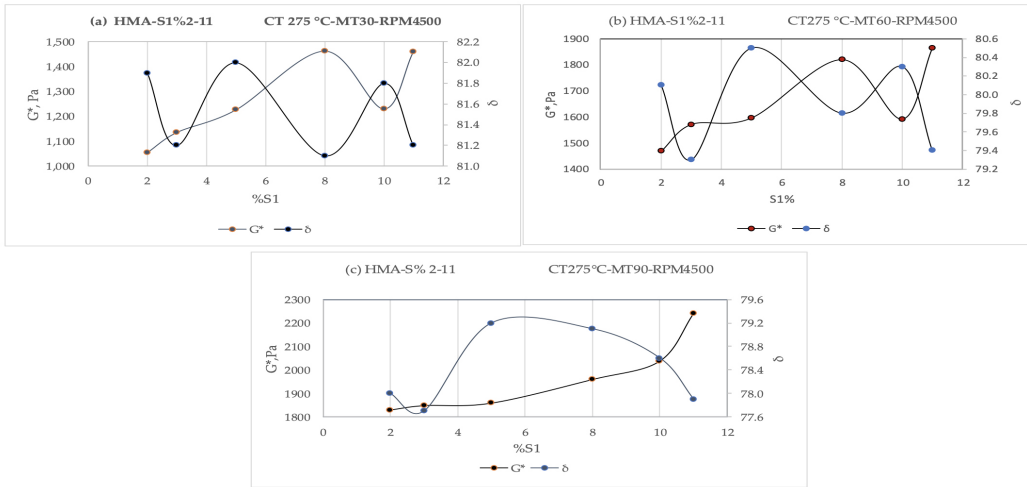


Figure 6. Evaluation of the results of viscoelastic parameters of improved HMA mixtures;  $G^*$ (Pa),  $\delta$  ( $^\circ$ ).

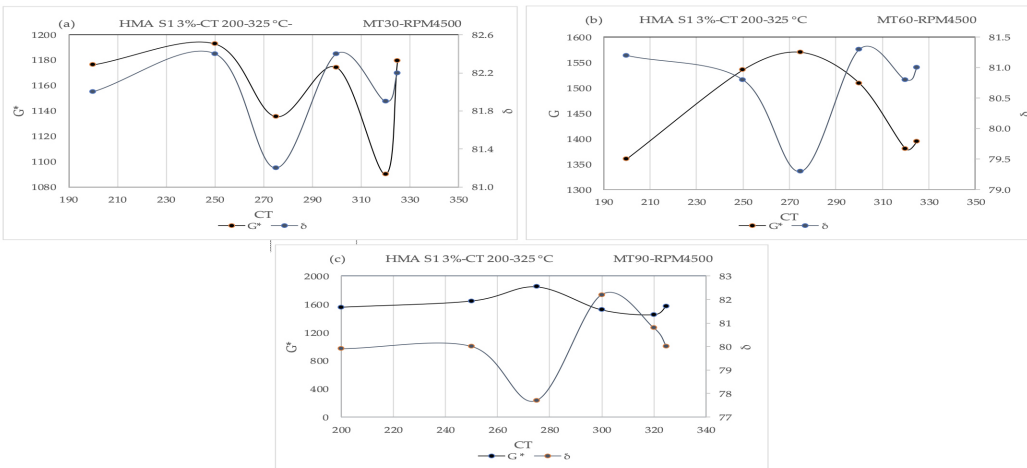


Figure 7. Evaluation of the results of viscoelastic parameters of improved HMA mixtures;  $G^*$ (Pa),  $\delta$  ( $^\circ$ ).

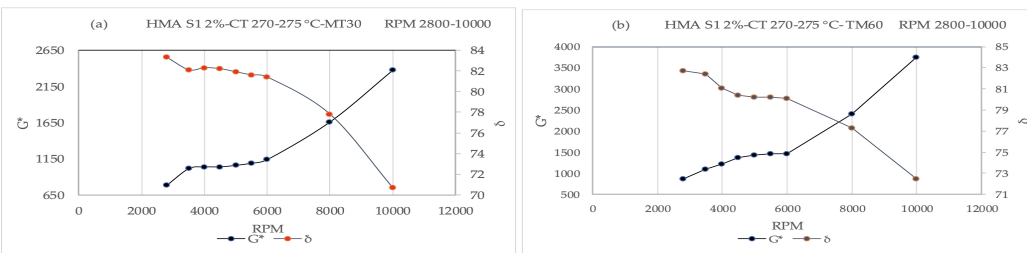


Figure 8. Variation of  $\delta$  and  $G^*$  with a) RPM and MT increase of 30 min; b) RPM and MT increase of 60 min.

properties, under the variation of operating parameters, demonstrated in the groups. HMA: I, II, III and IV mixtures. The theoretical basis is

the Langmuir isotherm, which is the first choice for most adsorption models and has many applications in surface kinetics (usually called

Langmuir-Hinshelwood kinetics) and thermodynamics. (Sultana *et al.*, 2017)

Table VI shows the results of the measurement of the

viscoelastic parameters of samples prepared with percentages of S1 additives in the proportions of 9, 10, and 11% by weight and with a mixing time of 120 minutes, maintaining the speed and constant HMA temperature at 4500rpm and 160°C. The DSR was maintained at temperatures of 76 and 82°C, and the Rutting factor in all cases exceeded 1kPa.

Table VII is obtained from Table V, which details the values of  $\Delta G^*$  and  $\Delta\delta$  that represent the differential of the value of  $G^*$  obtained between its values in MT(i),  $i = 30$  or  $90$  or  $120$  min. The magnitudes found represent the number of points that the variable  $G^*$  increased when it experienced an increase in the mixing time MT(i).

Calculation of the most efficient  $\Delta G^*$  value, due to the lower use of additive S1 (3%):

a) For MT (30), it corresponded to J with a value of 530.45Pa.

b) For MT (60), it corresponded to class J with a value of 965.65Pa.

c) For MT (90), it corresponded to class J with a value of 1244Pa.

The highest values of  $\Delta G^*$  selected from all HMA were:

d) For MT (30), it corresponded to class N with a value of 854.85Pa.

e) For MT (60), it corresponded to class N with a value of 1258.55Pa.

f) For MT (90), it corresponded to class N with a value of 1635.45Pa.

g) For MT (120), it corresponded to class N with a value of 2238.15Pa.

Consequently, it was shown that the HMA sample from class J with S1= 3% had better performance with a low percentage of additive; for MT values of 30, 60, and 90 minutes,  $G^*$  increased by 187.6%, 259.5%, and 305.5%, respectively; on the other hand, the HMA sample from class N with S1= 11% had the highest yield with a high percentage of additive for the MT of 30, 60, 90, and 120 minutes; the  $G^*$

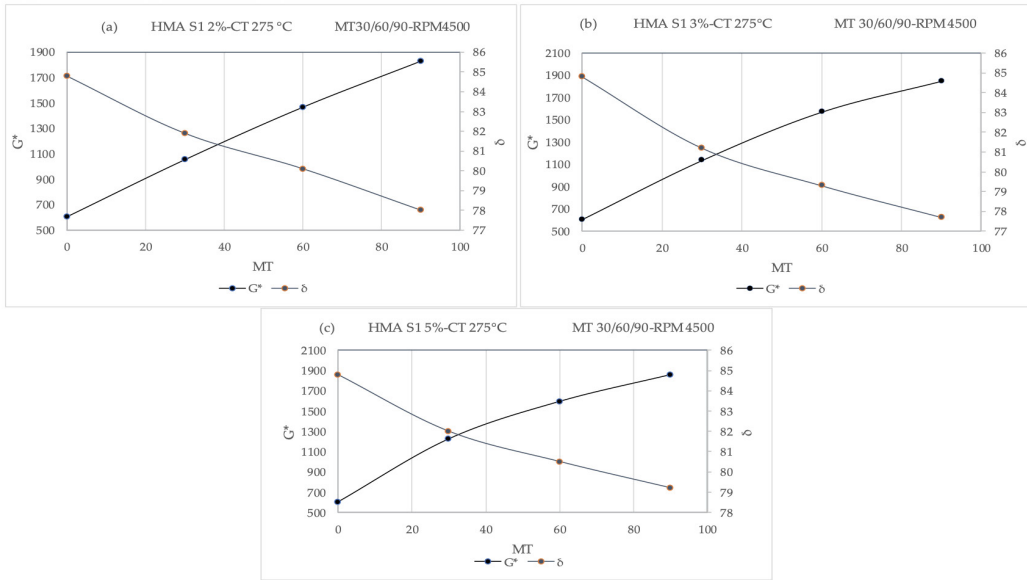


Figure 9. Variation of  $\delta$  and  $G^*$  with a) increase of MT 30-90 min and with S1= 2%; B) increase of MT 30-90 min and with S1= 3%; c) increase of MT 30-90 min and with S1= 5%.

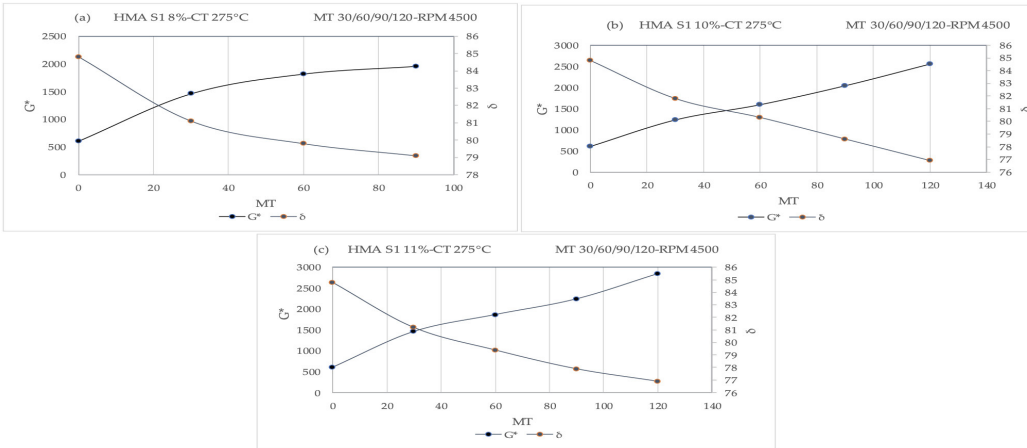


Figure 10. Variation of  $G^*$  and  $\delta$  with: a) increase of MT 30-90 min and with S1 = 8%; b) increase of MT 30-120.

TABLE VI  
MEASUREMENT OF PG 76 AND 82

Test °C (DSR)	$\delta(^{\circ})$	$G^*(Pa)$	$G^*/\text{sen}\delta(Pa)$	PG
76	78.7	1614.0	1645.9	76
76	77.5	1691.4	1732.5	76
76	76.8	1731.4	1778.4	76
82	72.7	1008.5	1056.3	82
82	72.1	1045.4	1098.6	82
82	71.6	1105.7	1165.3	82

$\delta(^{\circ})$ : Phase Angle;  $G^*(Pa)$ : Complex Module; PG: Performance Grade.

variable increased by 241%, 308%, 370%, and 470%, respectively. In all cases, the phase angle  $\delta$  decreased at a rate of approximately  $2.5^{\circ}$  per MT= 30 minutes of mixing. Consequently, the results showed that the HMA sample from group J is the final optimized mix, prepared with S1= 3%, RPM = 4500, CT= 275 °C, MT= 30, 60, 90 min, and a mixing temperature of 160°C. (Ezzat *et al.*, 2016).

The mixing time of 120 minutes may not be applicable in the industry due to high costs. Although the viscoelastic properties improve, but not substantially, to those achieved at 60 or 90 minutes, the mixing speeds should not be exceeded to prevent premature aging of the asphalt due to oxidation and thermal cracking.

## Conclusions

1. Ecuador has nanoclay deposits arranged in 6 levels, A1-A6, in an area of 4000 km<sup>2</sup>. The results of the nanometric evaluation of clay A1 gave the following results: a) a specific surface area of 280m<sup>2</sup>/gr; b) particle size between 50 and 250 nanometers; and c) high adsorption values shown in the respective tests, when calcined at 270 -275°C.

2. The nanoclays were treated with chemical and physical methods, using a) NaOH, b) NH<sub>3</sub>, H<sub>2</sub>O<sub>2</sub> (molar ratio 5), and c) controlled calcination to obtain the additive for the HMA, and 532 samples were prepared. Only the third method gave results that were representative and higher than the PRL reference level (PG= 70) in 84.8% and 3.2% in values higher than PG 76 and 82.

3. The type of nanoclay of choice was type A1, when it was calcined in the temperature window between 270-275°C, and the activation of its high adsorption capacity was achieved, which is why it became the additive S1. of choice. The essential modification of AC-20 asphalt with S1

TABLE VII  
POSITIVE VARIATION OF THE PARAMETERS G\* AND Δ BY CALCULATING ΔG\*, ΔΔ, AND PG

I		J		K	
ΔG*(Pa)	Δδ(°)	ΔG*(Pa)	Δδ(°)	ΔG*(Pa)	Δδ(°)
302.6%	-8.02%	305.5%	-8.37%	307.3%	-6.6%
G*/senδ PG=70		PG=70		PG=70	
L		M		N	
323.9%	-6.72%	421.7%	-9.32%	469.9%	-9.32%
G*/senδ PG=70,76		PG=70,76		PG=70,76,82	

is to come into contact immediately after calcination, to increase the use of this indicated property.

4. The integration of S1 in the AC-20 bitumen was optimized, testing different parameters and mixing times, CT, MT, RPM and %S. The best results were with CT= 275°C, MT= 90 min, RPM= 4500 and %S= 3% S1 additive, achieving 305.5% increase in G\*, while the phase angle δ decreased by -8.37%. HMA's performance rating improved from PG= 64 (original) to 70, 76 and 82; Additionally, there are promising results with mixing times of 30, 60 and 120 minutes.

#### REFERENCES

Airey GD, Rahimzadeh B, Andrew C (2004) Linear rheological Behavior of Bituminous Paving Materials. *Journal of Materials in Civil Engineering* 16: 212–220. [https://doi.org/10.1061/\(ASCE\)0899-1561\(2004\)16:3\(212\)](https://doi.org/10.1061/(ASCE)0899-1561(2004)16:3(212)).

Alshameri A, He H, Zhu J, Xi Y, Zhu R, Lingya Ma, Qi Tao (2018) Adsorption of Ammonium by Different Natural Clay Minerals: Characterization, Kinetics and Adsorption Isotherms. *Applied Clay Science* 159: 83–93. <https://doi.org/10.1016/j.clay.2017.11.007>.

Alujas A, Fernández R, Quintana R, Scrivener KL, Martirena F (2015) Pozzolanic Reactivity of Low Grade Kaolinitic Clays:

Influence of Calcination Temperature and Impact of Calcination Products on OPC Hydration. *Applied Clay Science* 108: 94–101. <https://doi.org/10.1016/j.clay.2015.01.028>.

Anon ND A (2023) AE500S-H Homogenizer High Shear Mixer Emulsifying Machine Digital Display (90G/60L): Amazon. Com: Tools & Home Improvement. <https://www.amazon.com/AE500S-H-Homogenizer-Emulsifying-Machine-Digital/dp/B079GKHWLL>

Anon ND B (2023) EBSCOhost | 54292474 | Engineering Properties of Nanoclay Modified Asphalt Concrete Mixtures.

Anon ND C (2023) Escuela Politécnica Nacional, Departamento de Metalurgia Extractiva (DEMEX). <https://www.epn.edu.ec/departamento-de-metalurgia-extractiva-demex/>.

Anon ND D (2023) Laboratorio de Control de Calidad de La Refinería Esmeraldas: Calidad En Sus Productos – EP PETROECUADOR. <https://www.epnetroecuador.ec/?p=4186>.

Anon ND E (2023) Muffle Furnace, Laboratory Muffle Furnace - Henan Sante Furnace Technical Co, Ltd. <https://www.saftherm.com/product/muffle-furnace/>.

Erol I (2016) Evaluation of Mechanical Properties of Nano-Clay Modified Asphalt Mixtures. *Measurement* 93: 359–371. <https://doi.org/10.1016/j.measurement.2016.07.045>.

Ezzat H, El-Badawy S, Alaa G, El Saaid Ibrahim Z, Tamer B (2016) Evaluation of Asphalt Binders Modified with Nanoclay and Nanosilica. *Procedia Engineering* 143: 1260–1267. <https://doi.org/10.1016/J.PROENG.2016.06.119>.

Firouzinia M, Shafabakhsh Gh (2018) Investigation of the Effect of Nano-Silica on Thermal Sensitivity of HMA Using Artificial Neural Network. *Construction and Building Materials* 170: 527–536. <https://doi.org/10.1016/j.conbuildmat.2018.03.067>.

Hakamy A, Shaikh FUA, Low IM (2015) Thermal and Mechanical Properties of NaOH Treated Hemp Fabric and Calcined Nanoclay-Reinforced Cement Nanocomposites. *Materials and Design* 80: 70–81. <https://doi.org/10.1016/j.matdes.2015.05.003>.

Hu W, Jia W, Zhu X, Gong H, Xue G, Huang B (2019) Investigating Key Factors of Intelligent Compaction for Asphalt Paving: A Comparative Case Study. *Construction and Building Materials* 229: 116876. <https://doi.org/10.1016/j.conbuildmat.2019.116876>.

Jahromi SG (2009) Estimation of Resistance to Moisture Destruction in Asphalt Mixtures. *Construction and Building Materials* 23: 2324–2331. <https://doi.org/10.1016/J.CONBUILDMAT.2008.11.007>

Kaufhold S, Kaufhold A, Jahn R, Brito S, Dohrmann R, Hoffmann R, Gliemann H, Weidler P, Frechen M. (2009) A

New Massive Deposit of Allophane Raw Material in Ecuador. *Clays and Clay Minerals* 57: 72–81. <https://doi.org/10.1346/CCMN.2009.0570107>

Mamuye Y, Chih Liao M, Duy Do N (2022) Nano-Al<sub>2</sub>O<sub>3</sub> Composite on Intermediate and High Temperature Properties of Neat and Modified Asphalt Binders and Their Effect on Hot Mix Asphalt Mixtures. *Construction and Building Materials* 331: 127304. <https://doi.org/10.1016/j.conbuildmat.2022.127304>.

Miller JS, William, Bellinger Y, United States Federal Highway Administration, Office of Infrastructure Research and Development (2003) *Distress Identification Manual for the Long-Term Pavement Performance Program* (Fourth Revised Edition). <https://doi.org/10.21949/1503647>

Onochie A, Fini E, Yang X, Mills-Beale J, You Z (2013) *Rheological Characterization of Nano-Particle Based Bio-Modified Binder*. <https://www.researchgate.net/publication/257292080>. (Cons. 06/26/2023).

Roberts FL, Kandhal PS, Brown RF, Lee DY, Kennedy TW (1996) *Hot Mix Asphalt Materials, Mixture Design and Construction*. National Asphalt Pavement Association Research and Education Foundation. Landham, USA. 603 pp. <https://trid.trb.org/view/473852>

Sultana N, Das A, Guria C, Hajra B, Chitres G, Saxena VK, Pathak AK (2017) Kinetics of Bentonite Nanoclay-Catalyzed Sal Oil (*Shorea Robusta*) Transesterification with Methanol. *Chemical Engineering Research and Design* 119: 263–285. <http://dx.doi.org/10.1016/j.cherd.2017.01.019>

Yao H, Zhanping Y, Li L, Shi X, Goh SW, Mills-Beale J, Wingard D (2012) Performance of Asphalt Binder Blended with Non-Modified and Polymer-Modified Nanoclay. *Construction and Building Materials* 35: 159–170. <https://doi.org/10.1016/j.conbuildmat.2012.02.056>.